INTERNATIONAL JOURNAL OF HYDROGEN ENERGY 39 (2014) 5858–5867

Available online at www.sciencedirect.com

ScienceDirect

journal homepage: www.elsevier.com/locate/he

Hydrogen sorption kinetics of La–Ni–Sn storage alloys

M.V. Blanco [a,b], E.M. Borzone [a,b], A. Baruj [a,c,*], G.O. Meyer [a,c]

[a] Centro Atómico Bariloche/Instituto Balseiro, CNEA/U. N. Cuyo, Av. Bustillo 9500, 8400 Bariloche, Argentina
[b] Agencia Nacional de Promoción Científica y Tecnológica (ANPCyT), Argentina
[c] Consejo Nacional de Investigaciones Científicas y Técnicas (CONICET), Argentina

ARTICLE INFO

Article history:
Received 18 November 2013
Received in revised form
10 January 2014
Accepted 20 January 2014
Available online 21 February 2014

Keywords:
Absorption kinetics
Metal hydride
Limiting mechanism
Purification

ABSTRACT

In this work we identify the limiting mechanism in the hydrogen absorption reaction of $LaNi_{5-x}Sn_x$ alloys. For this purpose the absorption reaction was modeled as a process involving several partial reactions occurring sequentially. The analysis was performed by comparing the experimental data with the descriptions derived from four different kinetic expressions, each considering that there is only one mechanism governing the hydrogen absorption reaction while the other steps occur near equilibrium conditions. Kinetic curves corresponding to the binary alloy $LaNi_5$ and to the substituted alloys $LaNi_{4.73}Sn_{0.27}$ and $LaNi_{4.55}Sn_{0.45}$ were measured using the Sieverts volumetric technique. Experiments were carried out over a temperature range from 300 K to 348 K and under different hydrogen pressures. In all cases, the best fit to the experimental data was achieved by applying an expression that assumes the limiting step of the overall reaction is the diffusion of hydrogen atoms through the hydride layer.

1. Introduction

The study of the hydrogen sorption reaction in hydride forming materials plays a key role in the design of storage and purification devices and heat-pump applications. Metal hydrides belonging to the AB_5 family have been widely studied because of their good reaction kinetics at room temperature, high cycling stability and good volumetric capacities. Partial substitutions of elements on the A and B sites allow the design of alloys that fulfil pressure and temperature requirements demanded by specific applications. As a consequence, these systems are used throughout a wide range of applications including hydrogen storage, compression, purification and rechargeable batteries [1,2]. In order to optimize devices design and to adequately model their performance it is necessary to fully characterize the alloy hydrogen reaction kinetics in the ranges of pressure and temperature that result of interest for specific operational conditions.

Many efforts have been made to study the underlying mechanisms of the reaction kinetics of AB_5 hydride forming alloys. In particular, several studies have focused in determining the kinetic mechanism governing the hydrogen absorption reaction. In this direction, hydrogen absorption curves corresponding to the $LaNi_5$, $LmNi_{4.91}Sn_{0.15}$ and $LaNi_{4.7}Al_{0.3}$ intermetallics have been modeled using the Johnson–Mehl–Avrami (JMA) and the Jander diffusion models [3]. JMA comprises both diffusion and nucleation and growth

* *Corresponding author*. Centro Atómico Bariloche, Av. Bustillo 9500, 8400 Bariloche, Argentina. Tel.: +54 294 4445278; fax: +54 294 4445299.
E-mail addresses: baruj@cab.cnea.gov.ar, baruj1@yahoo.com (A. Baruj).
0360-3199/$ – see front matter
http://dx.doi.org/10.1016/j.ijhydene.2014.01.125

as the limiting steps, while the Jander model only takes diffusion into account. The results indicated that the latter model was the best option for describing the process in all cases [3]. Payá and co-workers have also analyzed the mechanisms controlling the kinetics of absorption for $LaNi_5$ using JMA and the Crank–Nicholson diffusive model [4]. They found that both mechanisms were necessary to describe the reaction kinetics. While the initial 65% of the complete hydriding reaction fitted according to JMA, the final 35% was better described by the diffusive model. A different approach was taken by Dhaou et al. for the study of the reaction kinetics of $LaNi_5$, $LaNi_{4.85}Al_{0.15}$ and $LaNi_{4.75}Fe_{0.25}$ alloys [5]. According to these authors, after trying different possibilities they concluded that no existing kinetic model was satisfactory and instead preferred to derive empirical equations to describe the experimental data.

In order to gain more insight on the reaction mechanisms, Martin et al. have pointed out that neither the first-order reaction kinetics nor JMA equations are suited for describing the physics of the kinetics in metal-hydrogen systems [6]. Instead, they proposed a more detailed description in which the reaction follows five sequential steps and developed the corresponding mathematical descriptions. Each description assumes that only one step would limit the reaction. By applying this approach to $LaNi_{4.7}Al_{0.3}$ experimental results, they determined that the absorption reaction was controlled by surface chemisorption, whereas for the desorption process diffusion was found to be the limiting step. Fernández et al. applied the same model for the analysis of $MmNi_{4.7}Al_{0.3}$ hydrogen absorption kinetic [7]. They concluded that in the case of intentionally oxidized samples the reaction was dominated by surface processes, while for untreated and Pd-covered samples the kinetics was limited by diffusion. In a similar study [8], a combined model including all the partial reactions occurring during hydrogen absorption was developed. Furthermore, the model considered the case of transitional situations. The application of the model to the experimental kinetic curves of $LaNi_5$ showed good agreement with a reaction governed by a transition regime between diffusive and surface penetration mechanisms.

Using a similar approach, Smith and Goudy [9] applied the Shrinking Core Model (SCM) [10] for diffusion and chemical reaction controlling steps to study the dehydriding kinetics of the $LaNi_{5-x}Co_x$-H system. Results indicated that for $LaNi_5$ diffusion was the controlling step, while for $LaNi_4Co$, $LaNi_3Co_2$ and $LaNi_2Co_3$ the process was controlled by chemical reaction at the hydride-fresh material interface. In Ref. [11] the absorption kinetics of the $LaNi_{5-x}Al_x$ ($0 \leq x \leq 1.0$) system was studied by applying the kinetic models proposed by Chou [12]. In the cases of $LaNi_5$ and $LaNi_{4.7}Al_{0.3}$ the controlling mechanism was diffusion, while for $LaNi_4Al$ the best fit to the experimental data resulted from considering the surface penetration mechanism as the controlling step. In the case of $LaNi_5$, it was also found that the limiting step changed from diffusion to surface penetration when subjected to different pressures [11].

Considering all previous references it is clear that there is no prevalent model for analyzing hydrogen sorption kinetic results in AB_5 alloys. The main findings could be loosely summarized by saying that hydrogen absorption processes are dominated by diffusion mechanisms for $LaNi_5$ and related alloys with low Ni substitutions. However, for higher Ni replacement by other elements or under pressure changes, the absorption process can be governed by surface reactions.

Among AB_5 systems, $LaNi_{5-x}Sn_x$ alloys appear as a candidate for low pressure static applications. Although the thermodynamics, structure and microstructure of these compounds are well characterized in the literature [13–22], their reaction kinetics have not been extensively studied. Sato et al. studied the desorption kinetics of $LaNi_{4.8}Sn_{0.3}$ and estimated model coefficients by assuming diffusion as the limiting step [23]. Laurencelle et al. [19] presented an experimental kinetic study of $LaNi_{4.8}Sn_{0.2}$ and analyzed their results on the basis of a shrinking plate model characterized by an exponential dependence of the type $x_r = (1 - e^{-kt})$. In a recent work, we followed this approach in order to compare Laurencelle results with newly obtained data for several $LaNi_{5-x}Sn_x$ alloys [22]. The main finding was that Sn addition to $LaNi_5$ decreased the observed hydrogen absorption time. On one hand, those measurements were performed under the same external pressure conditions for different materials and driving force differences were not taken into account. On the other hand, the kind of approach used did not allow for an identification of the limiting mechanisms for the absorption process.

The purpose of the present paper is to identify the mechanisms governing the hydrogen absorption kinetics of $LaNi_{5-x}Sn_x$ compounds. We consider composition, temperature and external pressure variations in ranges of interest for hydrogen capture and purification applications. Analysis of the reaction of H_2 uptake is performed by comparing the experimental data with the different model descriptions.

2. Reaction model

2.1. Reaction stages

The hydrogen absorption process for an AB_5 alloy can be divided into several relevant stages [8]:

i. Hydrogen molecule in the gas moves to the surface of the intermetallic particle
ii. Hydrogen molecule is physisorbed at the solid surface of the particle
iii. Hydrogen molecule dissociates and hydrogen atoms are chemisorbed at the surface of the particle
iv. Hydrogen atoms penetrate through the surface of the particle
v. Hydrogen atoms diffuse through the hydride to the interface hydride/intermetallic
vi. Hydrogen atoms react with the intermetallic forming new hydride as product
vii. Hydrogen atoms diffuse through the α-metal phase

Stages i, ii and vii are usually not considered because, under normal operational conditions, they occur very quickly. For that reason, focus will be put on the other four processes, with the aim of determining which of them acts as the limiting stage in the hydrogen absorption reaction of the materials

presented. Analysis was made on assumption that there is only one mechanism controlling the reaction kinetics, while the rest occur near equilibrium conditions.

2.2. Surface reactions

Processes involved in steps (iii) and (iv) can be described by expressions derived from the unreacted shrinking core model (SCM) [10] and expressions proposed by Martin et al. [6]. The SCM considers a non-porous spherical particle in which the reaction takes place primarily at the outer surface. The reaction zone is expected to advance into the solid unreacted material leaving behind a completely transformed zone (Fig. 1). In this way, the core of unreacted material will decrease in size as the reaction proceeds.

In the case of the hydrogen absorption reaction, α is the metallic phase, β is the hydride phase, R is the radius of the particle (constant), r_c is the radius of the metal phase (unreacted core) which decreases with the advance of the reaction, and ξ is the reacted fraction. From geometric considerations, it can be written:

$$\xi = \frac{\frac{4}{3}\pi R^3 - \frac{4}{3}\pi r_c^3}{\frac{4}{3}\pi R^3} = 1 - \left(\frac{r_c}{R}\right)^3 \tag{1}$$

$$\frac{d\xi}{dt} = -\frac{3r_c^2}{R^3}\frac{dr_c}{dt} \tag{2}$$

Considering a dominant mechanism related to a phenomenon occurring at the surface of the particle (chemisorption or surface penetration), then the reaction would only be limited by the mass transfer through the outer surface of the particle, regardless of the size of the unreacted core.

The reacted fraction will be expressed as a function of the hydride front radial velocity dr_c/dt. As the reaction proceeds, dN_α moles of metal transform into hydride, thus decreasing the size of the α phase core:

$$dN_\alpha = \rho_\alpha dV = \rho_\alpha d\left(\frac{4}{3}\pi r_c^3\right) = 4\pi\rho_\alpha r_c^2 dr_c \tag{3}$$

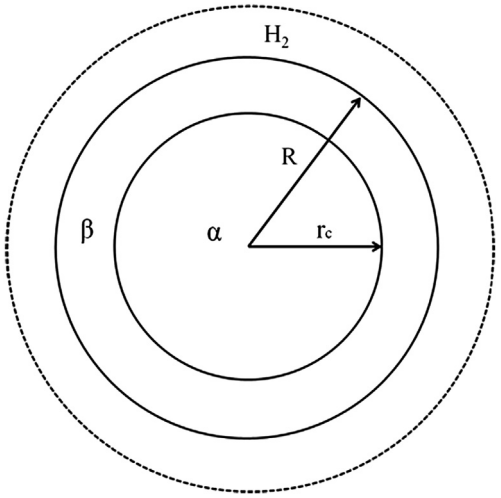

Fig. 1 – Unreacted shrinking core model scheme.

$$\frac{1}{S}\frac{dN_\alpha}{dt} = \frac{4\pi\rho_\alpha r_c^2}{4\pi R^2}\frac{dr_c}{dt} = \frac{\rho_\alpha r_c^2}{R^2}\frac{dr_c}{dt} \tag{4}$$

Here, ρ_α is the molar density of the metal phase, V is the volume of the particle and S is outer surface area of the particle.

2.2.1. Chemisorption

This stage considers that an already physisorbed hydrogen molecule dissociates as a result of the chemisorption reaction of individual hydrogen atoms with the particle surface. The rate per area unit $\dot{n}$ of hydrogen chemisorbed on the particle outer surface can be written as [6]:

$$\dot{n} = k_{ch}\left(p_{(t)} - p_{pl}\right) \tag{5}$$

Here, $p(t)$ is the external hydrogen pressure, p_{pl} is the plateau pressure during absorption and k_{ch} is the kinetic constant of the chemisorption process. Considering the hydride formation rate being proportional to the rate of hydrogen chemisorption on the surface of a spherical particle:

$$-\frac{1}{S}\frac{dN_\alpha}{dt} = k_{ch}\left(p_{(t)} - p_{pl}\right) \tag{6}$$

$$\frac{dr_c}{dt} = -\frac{R^2 k_{ch}}{\rho_\beta r_c^2}\left(p_{(t)} - p_{pl}\right) \tag{7}$$

Substituting Eq. (7) in Eq. (2), we have the final expression for a chemisorption dominated reaction:

$$\frac{d\xi}{dt} = \frac{3r_c^2}{R^3}\frac{R^2 k_{ch}}{\rho_\beta r_c^2}\left(p_{(t)} - p_{pl}\right) \tag{8}$$

2.2.2. Surface penetration

The stage of surface penetration considers the process where the hydrogen atoms pass from being chemisorbed on the outer surface of the particle into an absorbed state in the first sub-surface volume layers. In this case, the mass transfer rate can be written as [6]:

$$\dot{n} = k_{sp}\left(\sqrt{p_{(t)}} - \sqrt{p_{pl}}\right) \tag{9}$$

Here, k_{sp} is the kinetic constant of the hydrogen surface penetration process. Following a similar procedure to that applied on the chemisorption case, we find that the reaction rate for the case of a surface penetration governed reaction is given by:

$$\frac{d\xi}{dt} = \frac{3}{R}\frac{k_{sp}}{\rho_\beta}\left(\sqrt{p_{(t)}} - \sqrt{p_{pl}}\right) \tag{10}$$

2.3. Bulk reactions

Steps (v) and (vi) correspond to reactions limited by bulk processes. Bulk models assume the existence two phases at all times and do not describe the initial stages of the reaction where the hydride phase is nucleating. Transitions between different hydride phases are not considered [6].

2.3.1. Diffusion

The kinetic processes occurring in the bulk are described using the expressions proposed by Martin and co-workers [6].

Although Martin et al. described the reaction in terms of pressure changes, we have introduced a γ factor which allows describing the processes considering the variation of the reacted fraction. In the case of diffusion controlled kinetics, we have:

$$\Delta\xi = \frac{1}{\gamma}\Delta P \tag{11}$$

$$\gamma = \frac{\frac{4}{3}\pi\rho R_g T}{V_{ves}} \tag{12}$$

$$\left.\begin{aligned} \frac{d\xi}{dt} &= -A_D\gamma\left[\frac{\left(\frac{1}{\sqrt{p_{pl}}}-\frac{1}{\sqrt{p_{(t)}}}\right)}{\left(1-B\left(C-p_{(t)}\right)\right)^{-\frac{1}{3}}-1}\right] \\ A_D &= \frac{3DV_m\sqrt{k_D}n_{me}R_gT}{2R^2V_{ves}} \\ B &= \frac{2V_{ves}}{n_{me}R_gTZ} \end{aligned}\right\} \tag{13}$$

In Eq. (13), C is the initial pressure, D is the diffusion constant for hydrogen in the hydride phase, V_m is the molar volume of the hydride, k_D is the reaction constant of the diffusion process, n_{me} is the number of moles of the metal hydride phase, R_g is the universal gas constant, T is the temperature, V_{ves} is the volume of the vessel and Z is the stoichiometric factor of hydrogen in the hydride.

2.3.2. *Chemical reaction*

In the case of a process limited by the chemical reaction of hydrogen atoms at the boundary layer between the growing hydride and the shrinking metal phase, the expression can be written as [6]:

$$\left.\begin{aligned} \frac{d\xi}{dt} &= -A_{CR}\gamma\left(\frac{1}{\sqrt{p_{pl}}}-\frac{1}{\sqrt{p_{(t)}}}\right)\left(1-B\left(C-p_{(t)}\right)\right)^{\frac{2}{3}} \\ A_{CR} &= \frac{4\pi NR_gTk_rR^2}{2V_{ves}} \end{aligned}\right\} \tag{14}$$

Here, k_r is the reaction constant for the hydride formation process and the expression for B is the same as in Eq. (13). C is, again, the initial pressure.

The experimental data fitting procedures were performed using genetic algorithms [24–27].

3. Experimental procedure

$LaNi_{5-x}Sn_x$ alloys were prepared by arc-melting starting from the pure elements and then heat treated under an Ar atmosphere. The resulting alloys were confirmed to be single-phase by X-ray diffraction, presenting a P6/*mmm* symmetry for all samples. Chemical analysis was performed on each alloy by means of atomic absorption spectroscopy. Table 1 presents the alloy compositions, together with the designations that will be used from this point on in this paper. For details on the sample preparation procedure and the resulting characteristics of the alloys, see Ref. [22]. The equilibrium pressures for hydrogen absorption of these alloys are shown in Table 2.

During the process of measuring the data presented in this work, we have observed that it was absolutely essential to use freshly activated samples. When samples were kept under low vacuum conditions for a few hours, sorption kinetics deteriorated as it was previously observed and informed by Uchida et al. [28]. In order to prevent this deterioration and to ensure experimental reproducibility, each set of hydrogen absorption measurements was performed on a new fresh sample, immediately after its activation at the corresponding temperature.

The device used is a Sieverts type volumetric equipment developed at our laboratory in which the sample is contained in a 304L steel reactor. The reactor volume, of about 10 cm^3, has been previously calibrated. Volume calibration is also compensated for temperature effects in the measurements range. The samples, of about 0.35 g, are placed inside a 1 cm^3 cylindrical copper container which has a porous membrane on its base. The sample occupies about 10% of the vial volume. When measurements are performed, this cylinder lays horizontally and all of the sample powder is distributed on the lower part of the cylinder wall. The procedure for recording each absorption curve is as follows. In the initial state the sample is fully desorbed in a vacuum inside the reactor, with the temperature stabilized for at least 20 min. The measurement begins when this reactor is put in contact with a calibrated volume of about 80 cm^3, and filled with hydrogen at a determined pressure by opening a solenoid valve. From this point the composition data is calculated from the pressure drop in the system as usual. The system pressure is measured using a calibrated Baumer E914 transducer with a pressure range of 0–1600 kPa. The reactor temperature is regulated by means of a PID system with a 0.1 K step connected to a 200 W Watlow furnace. The sample temperature is measured by means of a Pt-100 sensor placed in contact with the outer wall of the reactor. Differences between the reactor outer and inner temperatures were corrected by applying an experimentally determined calibration curve. Temperature was set

Table 1 – Designation, nominal composition and measured chemical composition of the studied alloys. Values, expressed in atoms per unit formula, were measured by atomic absorption spectroscopy.

Alloy designation	Nominal composition	La (at.)	Ni (at.)	Sn (at.)
Sn00	$LaNi_5$	bal.	5.00	0.00
Sn01	$LaNi_{4.85}Sn_{0.15}$	bal.	4.82	0.18
Sn02	$LaNi_{4.75}Sn_{0.25}$	bal.	4.73	0.27
Sn03	$LaNi_{4.65}Sn_{0.35}$	bal.	4.66	0.34
Sn04	$LaNi_{4.55}Sn_{0.45}$	bal.	4.55	0.45
Sn05	$LaNi_{4.50}Sn_{0.50}$	bal.	4.49	0.51

Table 2 – Absorption equilibrium pressure (kPa) of the $LaNi_{5-x}Sn_x$ alloys, extracted from experimental van't Hoff plots for different temperatures [22].

Alloy designation	300 K	312 K	324 K	348 K
Sn00	274	406	596	1165
Sn01	71	114	181	410
Sn02	54	89	143	330
Sn03	44	73	120	287
Sn04	12	20	33	78
Sn05	5	9	15	38

at values between 300 K and 348 K. Experiment control and data acquisition were performed using a dedicated PC and a computer program developed in MS Visual Basic.

4. Results and discussion

4.1. Reaction kinetics of the $LaNi_{5-x}Sn_x$ system

The kinetics of hydrogen absorption and desorption for all samples were measured at 312 K and at an initial pressure of approximately 750 kPa. As it was previously mentioned, the absorption and desorption equilibrium pressures decrease as the grade of substitution of Ni by Sn increases. As a result, the absorption driving force related to the difference between the external pressure and the equilibrium pressure will be larger for the most substituted alloys. In Fig. 2a) it can be observed the improvement in absorption the kinetics from Sn00 to Sn05. As the substitution of Ni by Sn increases, the absorption curves present a better absorption performance.

Desorption measurements were performed at a back-pressure of less than 2 kPa. In this case, a decrease in the driving force from Sn00 to Sn05 at a fixed temperature and backpressure is expected. In this direction, alloys presenting lower equilibrium pressures will require more time to desorb than those having higher equilibrium pressure values. The kinetic curves of desorption of all the alloys are presented in Fig. 2b). It can be noticed a significant difference in the desorption kinetics from the binary to the substituted compounds.

From the viewpoint of technological applications, it would be convenient to have absorption and desorption processes taking place in comparable times. This condition is better met by alloys Sn00, Sn01 and Sn02, where the times required to complete the absorption and desorption reactions are comparable. On the other hand, for example, the time needed to achieve a full desorption for the Sn05 sample could turn this alloy in a very unsuitable option, even when it presents the best absorption kinetics. Ratnakumar and co-workers [29] addressed this problem and found that Sn compositions in the range of $0.2 \leq x \leq 0.3$ allowed achieving the optimal for high hydrogen capacities, long cyclic lifetime and improved reaction kinetics, while Sn substitutions within the range of $0.4 \leq x \leq 0.5$ were more appropriate for high temperature applications. We have then selected the alloys Sn02 and Sn04 in order to compare the mechanisms governing the absorption reaction kinetics with that of $LaNi_5$ (Sn00) when subjected to different temperature and pressure conditions.

4.2. Absorption kinetics at different temperatures

Although it is possible that throughout the different stages of the full hydrogen absorption reaction different processes could be acting as the limiting step [8], our objective is determining the main mechanism affecting the overall behavior. The present analysis is based on the assumption that only one process dominates the absorption behavior. Fitting of experimental data was carried out in the range of 0.2–0.8 of the reacted fraction where, according to previous measurements [22], the metal and hydride phases coexist. The initial parts of the kinetic curves, which include the solid solution region, were not fitted in order to avoid the possible misinterpretations stated by Martin et al. [6]. On the other end, the final parts of kinetic curves were left aside as they could be affected by the powder size distribution: while some bigger particles could be not fully hydrided and still be reacting, the smaller ones could have completed the phase transformation.

All four proposed models (stages (iii) to (vi)) were applied in order to evaluate the mechanism governing the kinetics of absorption of Sn00 at 300 K and 324 K. Fig. 3a) shows the results for 300 K. The selected initial external pressure was 469 kPa, in order to get the reaction completed at the end of the measurement. As it can be observed, the bulk models concerning hydrogen diffusion through the hydride layer mechanism (full line) and chemical reaction (dotted line) closely fit the experimental data. Descriptions based on surface reactions fail to describe the experimental values. In order to discern between both bulk models, an insert is presented inside the figure indicating the cumulative difference between the experimental reacted fraction and that obtained using the mathematical description for each case. From this analysis, the limiting step can be identified as diffusion.

Fig 3b) presents similar results for Sn00 at 324 K, hydrided under an initial external pressure of 985 kPa. Again, surface models do not provide adequate data fitting while bulk models are close to experimental results. An analysis based on

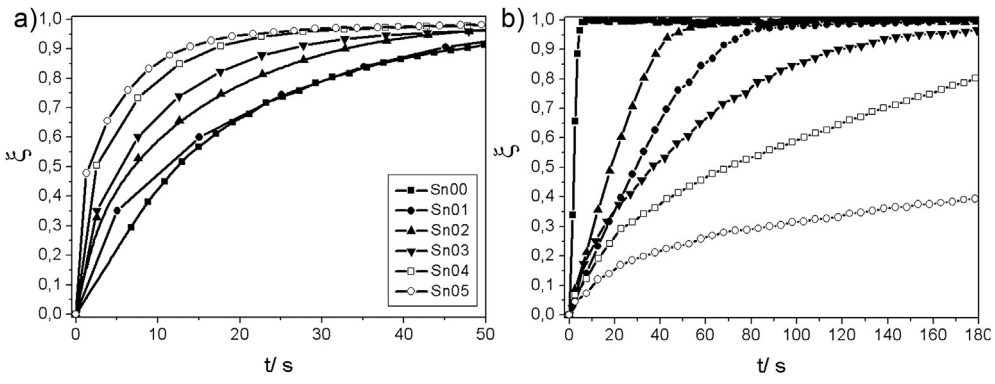

Fig. 2 – Reaction kinetics of $LaNi_{5-x}Sn_x$ ($0 \leq x \leq 0.5$) at 312 K a) Hydrogen absorption with an initial pressure of approximately 750 kPa b) Desorption at a maximum backpressure of 2 kPa.

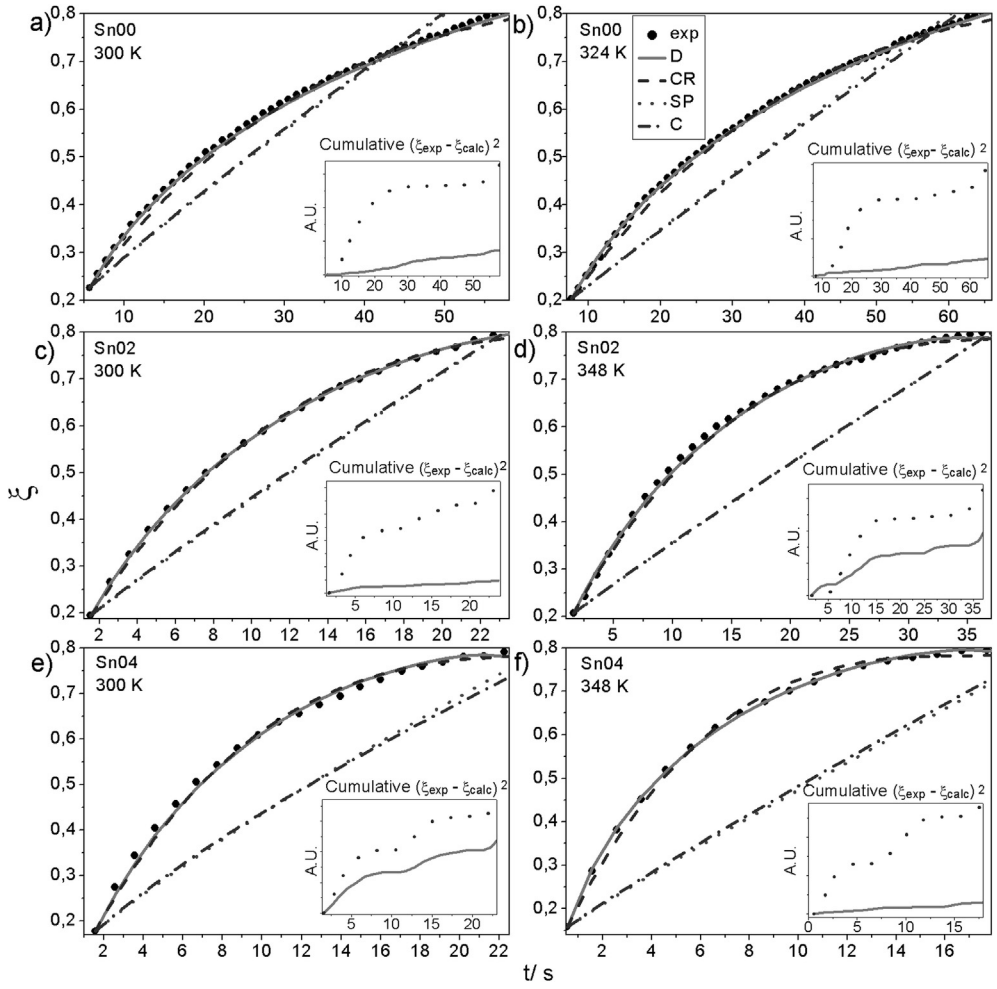

Fig. 3 – Adjustments to the experimental absorption curves of Sn00 at a) 300 K, b) 324 K; Sn02 at c) 300 K and d) 348 K; and Sn04 at e) 300 K, f) 348 K according to the diffusion model (D), chemical reaction model (CR), chemisorption model (C) and surface penetration model (PS).

differences shown in the inset again helps to identify diffusion as the limiting step. Although the selected range of temperatures is not very wide, it is representative of operational conditions for applications working near room temperature. Present results are in accordance with those reported in Refs. [4,9,11], which identified diffusion as the limiting step for the absorption kinetics of $LaNi_5$. A similar result, for a different AB_5 alloy, was also reported by Fernández et al. [7].

Fig. 3c) and d) show the results of applying the four proposed models to the absorption results of the substituted alloy Sn02 at 300 K and 348 K, respectively. The selected initial pressures for the measurements were 262 kPa (300 K) and 603 kPa (348 K), in order to get the reaction completed at the end of the measurement. As in the Sn00 case, the models corresponding to phenomena occurring in the bulk were the ones who achieved the best fittings to the experimental data. In both cases the diffusive model achieved the lower cumulative difference between the experimental data and the simulated results. Additional analyses were carried out over Sn02 absorption curves at 312 K and 324 K (not shown in the Figure) where the diffusive model also achieved the best fitting to the experimental data.

In Fig. 3e) and f) are shown the results of applying the four proposed models to the absorption results of Sn04 at 300 K and 348 K. The selected initial pressures for the measurements were 101 kPa (300 K) and 263 kPa (348 K). In both cases the diffusive model achieved the best fit to the experimental data. As in the case of Sn02, additional analyses were performed for absorption curves at 312 K and 324 K. The results were consistent with the diffusive model.

4.3. *Absorption kinetics at different initial external pressures*

There is evidence of changes in mechanisms associated with changes in external pressure in the hydriding kinetics of $LaNi_5$ and $LaNi_{4.7}Al_{0.3}$ alloys [11]. In order to analyze this possibility for $LaNi_{5-x}Sn_x$ alloys, we performed additional absorption kinetic measurements under different external pressures and temperatures for alloys Sn00, Sn02 and Sn04. The obtained curves were fitted according to the four proposed models and

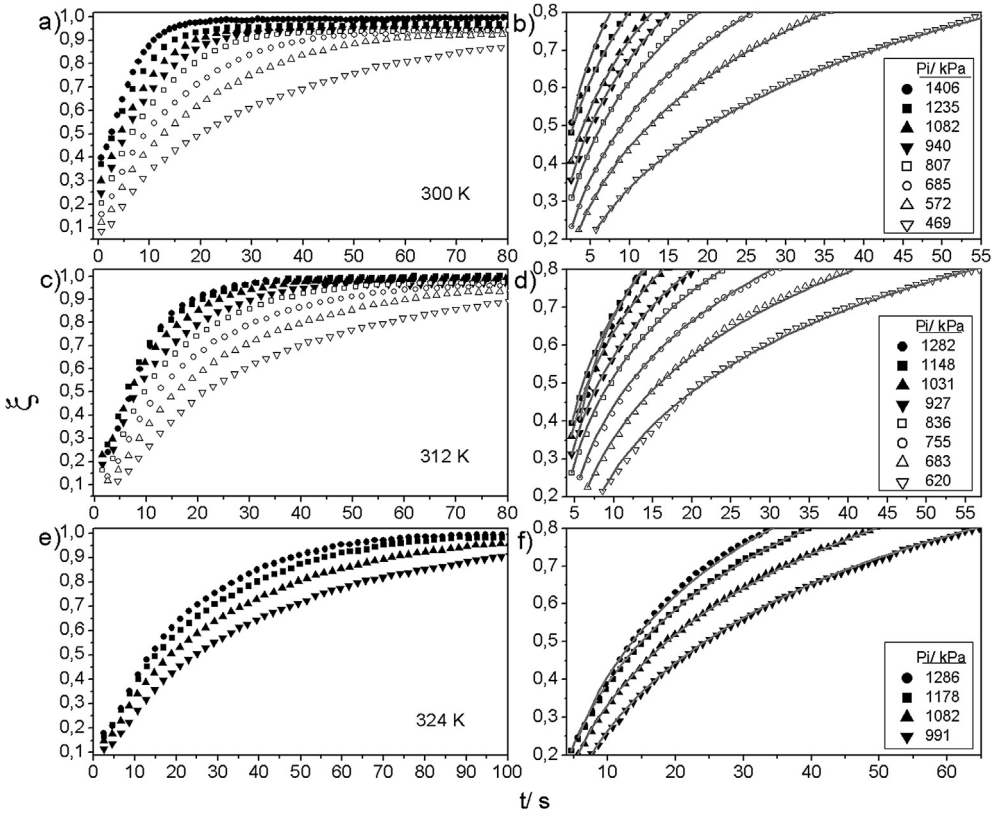

Fig. 4 – Reaction kinetics of $LaNi_5$ (Sn00) under different initial external pressures and temperatures. a,b) 300 K, c,d) 312 K and e,f) 324 K. Initial external pressures are indicated in the graphs labels for each temperature. Solid symbols correspond to experimental data, while full lines represent fits using the diffusive model.

an analysis of minimum squares was performed. For the sake of clarity only the results of the models which best described the experimental data will be shown.

In the case of alloy Sn00 ($LaNi_5$), absorption curves were obtained for temperatures of 300 K, 312 K and 324 K. At each selected temperature, kinetic measurements were performed under external pressures ranging from 469 kPa to 1406 kPa. The complete absorption curves are shown on the left side of Fig. 4. These kinetic curves were fitted according to the diffusive model in the range of the reacted fraction from 0.2 to 0.8. Curve fitting results are plotted on the right side of Fig. 4. The initial external pressure value for each curve is detailed within the graphs. As it can be noted, the diffusive model successfully described all the measured data.

The values of parameters A_D, B and C, as defined in Section 2.3.1, were obtained from the fittings. Parameter C can also be extracted from the experimental data because it corresponds to the initial external pressure. For the diffusive model, parameters A_D and B are expected to change with temperature and to be pressure independent. The parameter values obtained are summarized in Table 3.

In the case of the substituted alloy Sn02 ($LaNi_{4.73}Sn_{0.27}$), absorption curves were obtained for the temperatures of 300 K, 312 K, 324 K and 348 K and pressures ranging from 254 kPa to 1163 kPa. The experimental range is wider because the alloy reacts with hydrogen at lower pressures in comparison to $LaNi_5$. Analogous to the previous case, Fig. 5 shows on the left side the complete experimental absorption curves and the experimental data fitted according to the diffusive

Table 3 – Parameter values obtained from the best fitting to the experimental data shown in Fig. 5, applying the diffusion model to the absorption curves if Sn00, Sn02 and Sn04 (see, Section 2.3.1). Parameter C corresponds to the initial pressure in each case.

T/K	$LaNi_5$			$LaNi_{4.73}Sn_{0.27}$			$LaNi_{4.55}Sn_{0.45}$		
	A_D ($kPa^{3/2}$ s^{-1})	B($kPa^{1/3}$)	C(kPa)	A_D($kPa^{3/2}$ s^{-1})	B($kPa^{1/3}$)	C (kPa)	A_D($kPa^{3/2}$ s^{-1})	B($kPa^{1/3}$)	C (kPa)
300	24.64	0.0107	490–1426	11.62	0.0135	282–991	6.13	0.0174	120–426
312	31.55	0.0145	630–1294	14.48	0.0130	281–1143	10.52	0.0171	491–629
324	35.33	0.0117	1018–1311	32.72	0.0120	364–993	15.32	0.0169	373–607
348	–	–		54.44	0.0152	562–1163	32.79	0.0155	232–682

model on the right side. The model correctly describes the whole data set.

With regard to the analysis of the parameters values which achieved the best fittings to the experimental data (A_D, B and C) it is necessary to consider that the values of the stoichiometric factor might change from the binary to the substituted system. For this reason the value of parameter B is expected to change between $LaNi_5$ and $LaNi_{4.73}Sn_{0.27}$ samples. In Table 3 we summarized the values of parameters A_D, B and C.

In Fig. 6 are plotted the results of the fittings corresponding to the Sn04 ($LaNi_{4.55}Sn_{0.45}$) alloy at temperatures ranging from 300 K to 348 K for different initial external pressures. Again, the diffusive model describes accurately the experimental data.

Table 3 summarizes the values of the parameters corresponding to the best fit of the diffusive model to the experimental data. Values of parameters A_D and B remain constant at different hydrogen external pressures and are temperature dependent. On the other hand, when applying the chemical reaction method, large variations in the corresponding A_{CR} and B parameters as a function of pressure were found. These variations that could not be explained by the chemical reaction model, lend further support to the selection of diffusion as the limiting step for the studied conditions.

Considering the complete set of experimental results obtained for this work, diffusion through the hydride layer is the limiting mechanism for the hydrogen absorption reaction in the $LaNi_{5-x}Sn_x$ system. The main conclusion that can be derived from this observation is that the partial replacement of Ni by Sn does not have a significant impact over the surface properties of the alloys. This result is not obvious taking into account the role of Ni catalyzing the hydrogen molecule dissociation into individual atoms which, in principle, is not expected to be fulfilled by Sn. In addition, due to the difference between Sn and Ni atomic radii, the partial replacement of Ni by Sn in the $LaNi_{5-x}Sn_x$ system causes lattice distortion [14,16,22] and the appearance of crystalline defects [30]. In this context, diffusion paths for hydrogen atoms might be different in $LaNi_5$ in comparison to the substituted alloys thus leading to a faster diffusion through the hydride layer in the

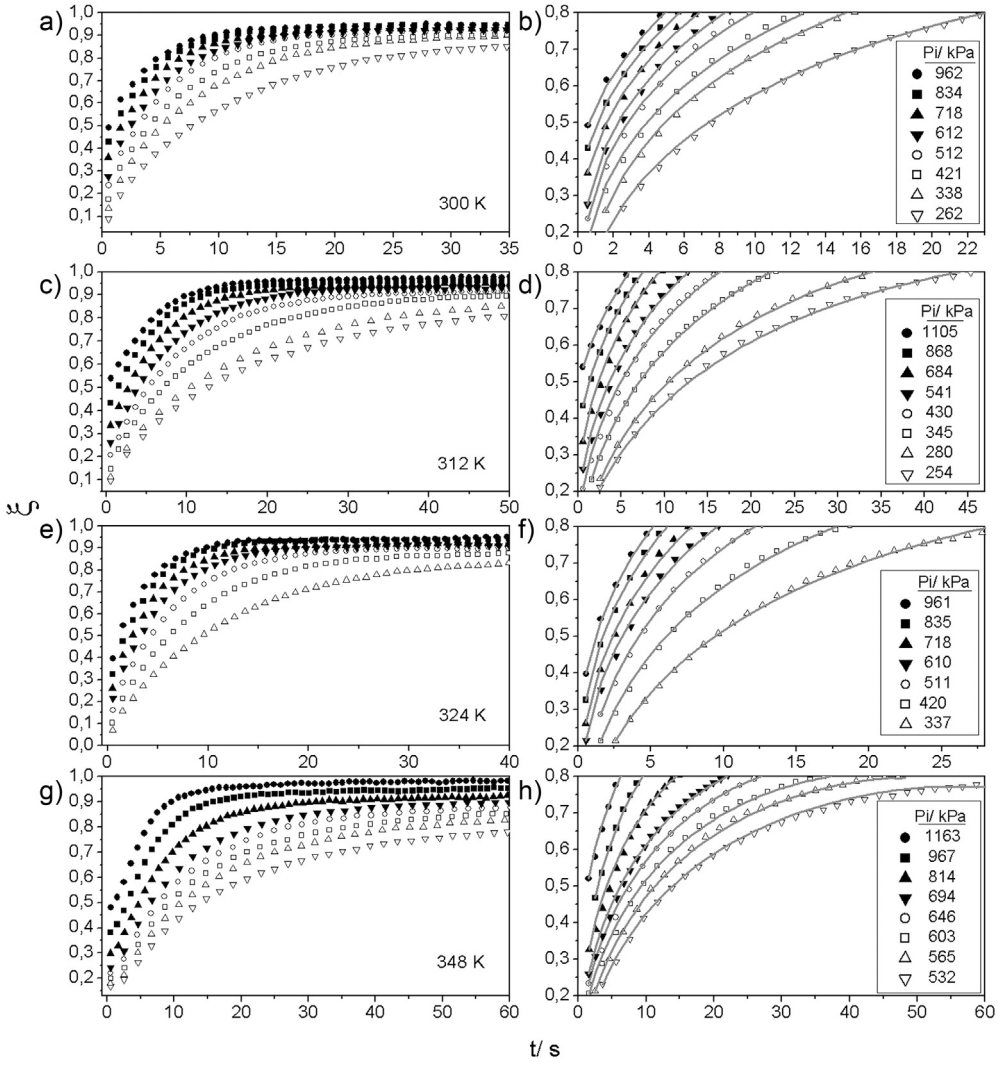

Fig. 5 – Reaction kinetics of $LaNi_{4.73}Sn_{0.27}$ under different initial external pressures and temperatures. a,b) 300 K, c,d) 312 K, e,f) 324 K and g,h) 348 K. Initial external pressures are indicated in the graphs labels for each temperature. Solid symbols correspond to experimental data, while full lines represent fits using the diffusive model.

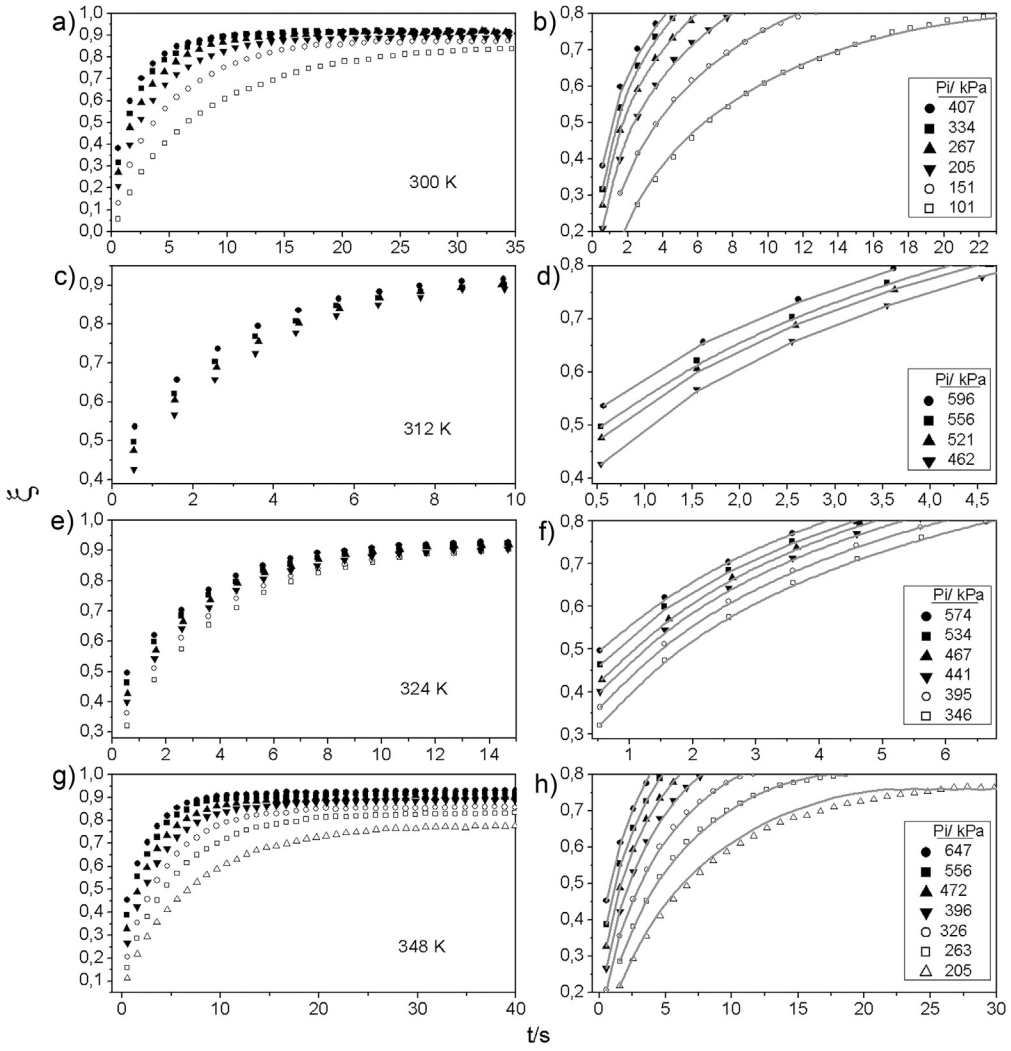

Fig. 6 – Reaction kinetics of $LaNi_{4.55}Sn_{0.45}$ (Sn04) under different initial external pressures and temperatures. a,b) 300 K, c,d) 312 K, e,f) 324 K and g,h) 348 K. Initial external pressures are indicated in the graphs labels for each temperature. Solid symbols correspond to experimental data, while full lines represent fits using the diffusive model.

latter cases. Nevertheless, this easier hydrogen diffusion in the hydride of ternary alloys is not efficient enough to change the limiting mechanism for the reaction. Although the limiting stage in the hydride absorption reaction of the $LaNi_5$ compound partially substituted by Sn has not been previously reported in the literature, a change in the mechanism governing the desorption kinetics between $LaNi_5$ and $LaNi_{5-x}Co_x$ was found by Smith et al. [9]. In that case, the addition of Co caused the limiting mechanism to change from diffusion to chemical reaction at the hydride/metal boundary. This observation could be taken as a precedent about changes in limiting mechanisms from binary to substituted systems. However, this kind of change was not observed for the $LaNi_{5-x}Sn_x$ system in the composition range under study.

Another useful observation was the strong effect of surface contamination over the hydrogen reaction kinetics of $LaNi_{5-x}Sn_x$ alloys. As it was mentioned in Section 3, noticeable changes in the kinetics were detected when samples stayed a few hours under low (mechanical pump) vacuum. Although results were not presented here for the sake of clarity, in such cases surface penetration was found to be as important as diffusion as the limiting stage. We are currently exploring this aspect of $LaNi_{5-x}Sn_x$ alloys, and results will be presented in a forthcoming contribution.

5. Conclusions

In this work we studied the kinetic mechanisms governing the hydrogen absorption reaction of the alloys belonging to the $LaNi_{5-x}Sn_x$ ($0 \leq x \leq 0.5$) system. The analysis was performed on the basis of four mathematical models, each of them representative of a kinetic mechanism: chemisorption, surface penetration, diffusion and chemical reaction. The analyses were performed over the binary alloy $LaNi_5$ and two Sn-substituted alloys, $LaNi_{4.73}Sn_{0.27}$ and $LaNi_{4.55}Sn_{0.45}$, in order to study if there was any effect of the Sn content on the rate-limiting step of the hydrogen absorption reaction.

Measurements were carried out for each of these alloys at different temperatures ranging from 300 K to 348 K, and at

different hydrogen external pressures. All the obtained curves were fitted according to the four proposed models.

In the case of the binary alloy, it was concluded that the overall absorption reaction was limited by the process of diffusion of hydrogen atoms through the hydride layer. This result was in accordance with previously reported studies. Values of the parameters involved in the diffusive model were obtained in each case. With regard to the substituted systems, both of them presented a kinetic behavior that could also be explained by applying the diffusive model. The values of the parameters involved were presented for each alloy at different temperatures. The values were expected to differ from the binary to the substituted systems and within the substituted systems because the diffusive coefficient and the stoichiometric factor may have different values. At each temperature, the values of parameters A_D and B, which are pressure independent, remained constant for the different external hydrogen pressures, supporting the consistency of the model.

Acknowledgments

The authors gratefully acknowledge the financial support from ANPCyT (PAE 36985, PAE-PICT 2007-00158 and PFDT-PRH 200). Silvia Rivas, Facundo Roldán and Enrique Aburto kindly helped with equipment construction and the preparation of samples. Claudia Osuna helped with chemical characterization of materials.

REFERENCES

[1] Sandrock G. A panoramic overview of hydrogen storage alloys from a gas reaction point of view. J Alloys Compd 1999;293–295:877–88.
[2] Sakituna B, Lamari-Darkrim F, Hirscher M. Metal hydride materials for solid hydrogen storage: a review. Int J Hydrogen Energy 2007;32:1121–40.
[3] Muthukumar P, Satheesh A, Linder M, Mertz R, Groll M. Studies on hydriding kinetics of some La-based metal hydride alloys. Int J Hydrogen Energy 2009;34:7253–62.
[4] Payá J, Freni A, Corberán JM, Compañ V. Hydriding kinetics of $LaNi_5$ using nucleation-growth and diffusion models. J New Mater Electrochem Syst 2012;15:293–300.
[5] Dhaou H, Askri F, Ben Salah M, Jemni A, Ben Nasrallah S, Lamloumi J. Measurement and modelling of kinetics of hydrogen sorption by $LaNi_5$ and two related pseudobinary compounds. Int J Hydrogen Energy 2007;32:576–87.
[6] Martin M, Gommel C, Borkhart C, Fromm E. Absorption and desorption kinetics of hydrogen storage alloys. J Alloys Compd 1996;238:193–201.
[7] Fernández GE, Rodríguez D, Meyer G. Hydrogen absorption kinetics of $MmNi_{4.7}Al_{0.3}$. Int J Hydrogen Energy 1998;23:1193–6.
[8] Schweppe F, Martin M, Fromm E. Model on hydride formation describing surface control, diffusion control and transition regions. J Alloys Compd 1997;261:254–8.
[9] Smith G, Goudy AJ. Thermodynamics, kinetics and modeling studies of the $LaNi_{5-x}Co_x$ hydride system. J Alloys Compd 2001;316:93–8.
[10] Levenspiel O. Chemical reaction engineering. 3rd ed. Hoboken: Wiley; 1999.
[11] An XH, Pan YB, Luo Q, Zhang X, Zhang JY, Li Q. Application of a new kinetic model for the hydriding kinetics of $LaNi_{5-x}Al_x$ ($0 \leq x \leq 1.0$) alloys. J Alloys Compd 2010;506:63–9.
[12] Chou Kuo-Chih, Xu Kuangdi. A new model for hydriding and dehydriding reactions in intermetallics. Int J Hydrogen Energy 2007;15:767–77.
[13] Lambert SW, Chandra D, Cathey WN, Lynch FE, Bowman Jr RC. Investigation of hydriding properties of $LaNi_{4.8}Sn_{0.2}$, $LaNi_{4.27}Sn_{0.24}$ and $La_{0.9}Gd_{0.1}Ni_5$ after thermal cycling and aging. J Alloys Compd 1992;187:113–35.
[14] Cantrell JS, Beiter TA, Bowman Jr RC. Crystal structure and hydriding behavior of $LaNi_{5-y}Sn_y$. J Alloys Compd 1994;207–208:372–6.
[15] Luo S, Luo W, Clewley JD, Flanagan TB, Wade LA. Thermodynamic studies of the $LaNi_{5-x}Sn_x$-H system from $x = 0$ to 0.5. J Alloys Compd 1995;231:467–72.
[16] Luo S, Clewley JD, Flanagan TB, Bowman Jr RC, Wade LA. Further studies of the isotherms of $LaNi_{5-x}Sn_x - H$ for $x = 0$–0.5. J Alloys Compd 1998;267:171–81.
[17] Joubert JM, Latroche M, Černý R, Bowman Jr RC, Percheron-Guégan A, Yvon K. Crystallographic study of $LaNi_{5-x}Sn_x$ ($0.2 \leq x \leq 0.5$) compounds and their hydrides. J Alloys Compd 1999;293–295:124–9.
[18] Fultz B, Witham CK, Udovic TJ. Distributions of hydrogen and strains in $LaNi_5$ and $LaNi_{4.75}Sn_{0.25}$. J Alloys Compd 2002;335:165–75.
[19] Laurencelle F, Dehouche Z, Goyette J. Hydrogen sorption cycling performance of $LaNi_{4.8}Sn_{0.2}$. J Alloys Compd 2006;424:266–71.
[20] Nakamura Y, Nakamura J, Iwase K, Akiba E. Distribution of hydrogen in metal hydrides studied by *in situ* powder neutron diffraction. Nucl Instrum Methods Phys Res A 2009;600:297–300.
[21] Sakaki K, Date R, Mizuno M, Araki H, Nakamura Y, Shirai Y, et al. Behavior of vacancy formation and recovery during hydrogenation cycles in $LaNi_{4.93}Sn_{0.27}$. J Alloys Compd 2009;477:205–11.
[22] Borzone EM, Baruj A, Blanco MV, Meyer GO. Dynamic measurements of hydrogen reaction with $LaNi_{5-x}Sn_x$ alloys. Int J Hydrogen Energy 2013;38:7335–43.
[23] Sato M, Stange M, Yartys VA. Desorption behaviour of hydrogen in the $LaNi_{4.7}Sn_{0.3}$-H system. J Alloys Compd 1995;396:197–201.
[24] Gulsen M, Smith AE, Tate DM. A genetic algorithm approach to curve fitting. Int J Prod Res 1995;33:1911–23.
[25] Tinós R, Yang S. A self-organizing random inmigrants genetic algorithm for dynamic optimization problems. Genet Program Evolvable Mach 2007;8:255–86.
[26] Misevicius A. An improved hybrid genetic algorithm: new results for the quadratic assignment problem. Knowl Based Syst 2004;17:65–73.
[27] Katare S, Bhan A, Caruthers JM, Delgass WN, Venkatasubramanian V. A hybrid genetic algorithm for efficient parameter estimation of large kinetic models. Comput Chem Eng 2004;28:2569–81.
[28] Uchida H, Seki S, Seta S. Effect of surface contamination on the hydriding behaviors of $LaNi_{4.5}Al_{0.5}$, $LaNi_{2.5}Co_{2.5}$ and $LaNi_{4.5}Mn_{0.5}$. J Alloys Compd 1995;231:403–10.
[29] Ratnakumar BV. Electrochemical studies on $LaNi_{5-x}Sn_x$ metal hydride alloys. J Electrochem Soc 1996;143:2578–84.
[30] Matsuda J, Nakamura Y, Akiba E. Lattice defects introduced into $LaNi_5$-based alloys during hydrogen absorption/desorption cycling. J Alloys Compd 2011;509:7498–503.